Ring-opening metathesis polymerization of norbornene-benzoladderene (macro)monomers

*Samantha J. Scannelli, Mohammed Alaboalirat, Diego Troya, and John B. Matson**

Department of Chemistry, Virginia Tech, Blacksburg, VA 24061, United States
Macromolecules Innovation Institute, Virginia Tech, Blacksburg, VA 24061, United States
*Correspondence: jbmatson@vt.edu

KEYWORDS: Ruthenium catalyst, Grafting-through, Copolymerization, ^{1}H NMR spectroscopy, Size exclusion chromatography

For Table of Contents use only:

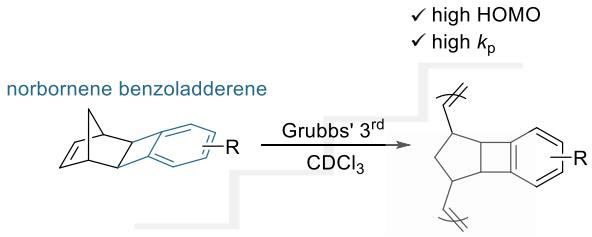

We report high k_p (macro)monomer structures for use in grafting-through ring-opening metathesis polymerization to make linear and bottlebrush polymers.

Abstract

Norbornene-based monomers are common starting points in ring-opening metathesis polymerization (ROMP) due to their high ring strain, and recent reports highlight how the structure of norbornene derivatives influences polymerization rates. In particular, the anchor group, the series of atoms directly connected to the norbornene, critically affects polymerization. In this work, we introduce a new anchor group, the *exo*-norbornene-benzoladderene (NBL), for use in ROMP. We synthesized one small molecule NBL monomer and two polystyrene (PS) macromonomers (MMs), each containing a polystyrene side-chain, varying the position where the side-chain was attached to the anchor group arene ring. We then evaluated propagation rate constants (k_p) and examined their correlation with calculated HOMO energies using density functional theory. The small molecule monomer and the MM with the PS side-chain in the *meta* position had high k_p values, consistent with the high HOMO energies of the anchor groups, a predictor of k_p. Conversely, when the side-chain was in the *ortho* position, closer to the reactive olefin, k_p was 3.3-fold lower than the *meta*-MM. We hypothesized that the unexpectedly slow polymerization of the *ortho*-MM was due to steric interference between the growing bottlebrush side-chains and the coordinating MM, resulting in a lower k_p than predicted. In copolymerization studies of these MMs with a small molecule diluent monomer, we found a negligible difference in the MM propagation rate between the two MMs, supporting our hypothesis. Ultimately, the introduction of the NBL structure as an anchor group broadens the scope of (macro)monomer structures available for ROMP.

Introduction

Ring-opening metathesis polymerization (ROMP) has garnered interest in recent years as a robust method to synthesize complex polymer architectures, such as bottlebrush polymers.[1-3] Specifically, ROMP is widely utilized to polymerize macromonomers (MMs), in a technique called the grafting-through approach, resulting in bottlebrush polymers with 100% side-chain grafting density (i.e., $z = 1$) along the backbone.[1, 4-6] Mediated by highly active Ru catalysts, such as Grubbs' third-generation catalyst [G3, $(H_2IMes)(Cl)_2(pyr)_2RuCHPh$], ROMP exhibits living characteristics.[7-8] High livingness in ROMP allows for control over the molecular weight and dispersity ($Đ$) of the resulting polymers, which is particularly critical for the synthesis of well-defined bottlebrush polymers due to the sterically demanding nature of MMs.[9-10]

Unlike many other polymerization techniques, ROMP has relatively low sensitivity to air and water, enabling its use on the benchtop in many cases. ROMP can have high functional group tolerance, allowing for the direct polymerization of functional monomers and MMs.[11-15] In recent years there has been interest in broadening the scope of (macro)monomers used in ROMP to achieve faster polymerizations, as well as larger and better-defined polymers.[16-23] A common cyclic olefin used in ROMP is norbornene, often with substituents, due to its high ring strain providing high propagation rates (k_p) and its facile functionalization with various side chains to make MMs.[24-27] By tuning the side-chain identities and sizes to match specific applications, researchers have turned to ROMP to synthesize various bottlebrush polymers for use in several areas, including as nanomaterials with unusual shapes,[28-30] photonic crystals,[31-33] organic electronic materials,[34-36] elastomers,[37-39] and in biomedical systems.[40-44] However, continued development of MM structures and their successful ROMP is needed to synthesize novel bottlebrush polymer materials to continue to expand potential applications of this polymer class.

Design of new bottlebrush polymers mostly focuses on the inclusion of diverse polymer side-chains along the backbone to achieve unique properties or behavior in the resultant material. However, development of the anchor group, the series of atoms connecting the polymerizable unit (e.g., norbornene) to a functional group or polymer side-chain,[45] can also help improve reproducibility in bottlebrush polymers synthesis and structural integrity in bottlebrush (multi)block copolymers. Not only is the anchor group important as the linker between the backbone and side-chains of bottlebrush polymers, but it also greatly affects the reactivity of the norbornene unit.[25, 46-47] Our group has studied the effects of the anchor group in ROMP, and we have found that the energy of the HOMO centered on the norbornene olefin of various (macro)monomer structures is a reasonable predictor for olefin reactivity, showing a positive correlation with k_p values.[48-49] Therefore, development and characterization of new anchor groups broadens the scope of bottlebrush polymer materials by increasing (macro)monomer structural diversity and allowing for tunability of monomer olefin reactivity.

Here, we designed an *exo*-norbornene-benzoladderene (NBL) anchor group for use in ROMP of (macro)monomers. This anchor group was inspired by work from Xia and coworkers, who developed the efficient catalytic arene-norbornene annulation (CANAL) method to synthesize ladder polymers.[50-52] Their interest was expanding the synthetic methods used to generate rigid ladder polymers and in developing a new class of ladder polymers from easily accessible monomers.[53] In this work, we envisioned that the CANAL reaction could be used to synthesize novel norbornene-based (macro)monomers with a rigid anchor group. We synthesized and evaluated three related NBL compounds, one small molecule monomer and two MMs, to be used in ROMP to prepare linear and bottlebrush polymers, respectively. Between the two MMs, we envisioned that varying the position where the side-chain was attached to the anchor group would

allow us to probe how regiochemistry on the arene ring influenced k_p. Additionally, we aimed to compare k_p values for these NBL compounds to other more commonly used (macro)monomers to highlight the importance of continued development of anchor group structures.

Results and Discussion

First, we aimed to synthesize an NBL monomer for use in the synthesis of linear polymers by ROMP. Anchor groups in the *exo* configuration have superior ROMP kinetics to those in the *endo* configuration, with k_p values for *exo* monomers typically 10–100-fold higher than those for *endo* monomers.[54-55] Therefore, studying this new anchor group in the *exo* configuration was important for enhanced propagation rates. We utilized a method reported by Xia and coworkers for the synthesis of NBL compounds with exclusive selectivity for the *exo* product (abbreviated *xx* to indicate *exo* stereochemistry at the 5 and 6 positions).[52] Scheme 1 depicts the synthesis of monomer *xx*-NBL (**1**). In brief, an annulation reaction between norbornadiene and 4-bromotoluene, mediated by a Pd catalyst, afforded the desired product. CANAL has primarily been used as a polymerization technique between norbornadiene and dibromoarene monomers; therefore, consideration of reactant choice and equivalents was important. An excess of norbornadiene was required to minimize annulation on both sides of the norbornadiene ring, and we used mono-brominated arenes to avoid polycondensation. Despite these efforts, inevitable disubstitution on norbornadiene led to poor to fair yields of the target monosubstituted product, suggesting that the second annulation reaction is faster than the first. Despite this, we were able to isolate sufficient quantities of monomer *xx*-NBL (**1**), and we envision that more optimized conditions that reduce the rate of the second reaction, for example by coordinating one of the alkenes with a Lewis acid, could improve yields.

Scheme 1. Synthesis of *exo*-norbornene-benzoladderene monomer [*xx*-NBL (**1**)][a]

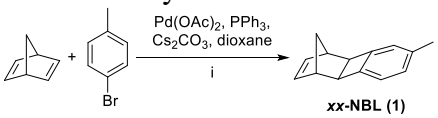

[a]NBL monomer with *exo-exo* (*xx* prefix) stereochemistry. Conditions: (i) Reflux, 12 h, 24%.

This general CANAL reaction, under similar conditions, was used to synthesize two MM structures for use in ROMP to make bottlebrush polymers. We designed both *xx*-NBL structures as initiators for atom transfer radical polymerization (ATRP). The position of the α-bromoester ATRP initiator varied on the arene ring (Scheme 2). CANAL of 2-bromobenzyl alcohol protected with tetrahydro-2*H*-pyran (compound **I**) formed the precursor *xx*-NBL structure (compound **II**, Scheme 2A). Removal of the protecting group (compound **III**) and reaction with bromoisobutyryl bromide afforded ATRP initiator ***xx*-NBL-*o*-Br**. The *ortho* positioning of the two functionalities on the benzene ring in compound **I** forced annulation to occur at only one position, eliminating isomeric products. To place the α-bromoester in the *meta* position, methyl 4-bromo-3-methylbenzoate (compound **IV**) was used in the CANAL reaction (Scheme 2B). The methyl substituent was necessary to force annulation at only one position on the ring, avoiding a complex mixture of products that formed when the methyl group was omitted. Reduction of the methyl ester (compound **V**) to form the benzyl alcohol (compound **VI**) followed by installation of the α-bromoester group afforded ATRP initiator ***xx*-NBL-*m*-Br**.

Scheme 2. Synthesis of *xx*-NBL ATRP initiator compounds[a]

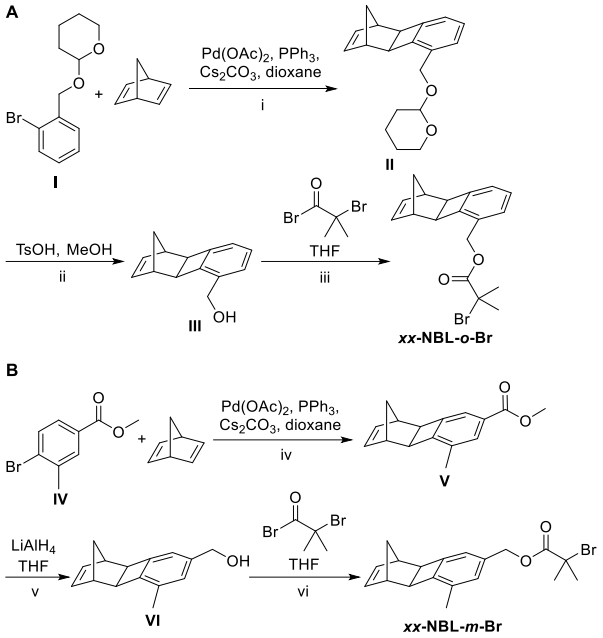

[a]All NBL compounds exhibited *exo-exo* (*xx* prefix) stereochemistry. Italicized letters identify the position of substitution on the arene ring starting from the top left carbon of the ring (*o* = *ortho* and *m* = *meta*). Conditions: (i) Reflux, 12 h, 15%; (ii) rt, 2 h, >99%; (iii) rt, 12 h, 42%; (iv) reflux, 12 h, 40%; (v) rt, 12 h, 67%; (vi) reflux, 16 h, 40%.

Next, we employed ATRP to add a polystyrene (PS) side-chain to both ATRP initiators. We targeted number-average molecular weight values (M_n) of approximately 3 kg/mol for both MMs. All ATRP reactions were performed under typical conditions for styrene at 90 °C for 3 h. During ATRP, styrene can undergo undesired side reactions, including copolymerization with norbornene and termination by combination at high monomer conversion.[56-57] To reduce the incidence of these side reactions with the goal of avoiding branched and coupled bottlebrush polymer products, we targeted low styrene conversion (10%) in the ATRP steps. The resulting crude MMs were then diluted with water and extracted with ethyl acetate before precipitation into MeOH four times to yield the pure MM products as white powders. The final MM products were then analyzed by size exclusion chromatography (SEC) to determine M_n and dispersity ($Đ$). MM *xx*-NBL-*o*-PS (**2**) had an M_n value of 2.9 kg/mol with a $Đ$ value of 1.04 and MM *xx*-NBL-*m*-PS (**3**) had an M_n of 3.0 kg/mol and a $Đ$ value of 1.06 (Scheme 3).

Scheme 3. ATRP to synthesize *xx*-NBL-based MMs[a]

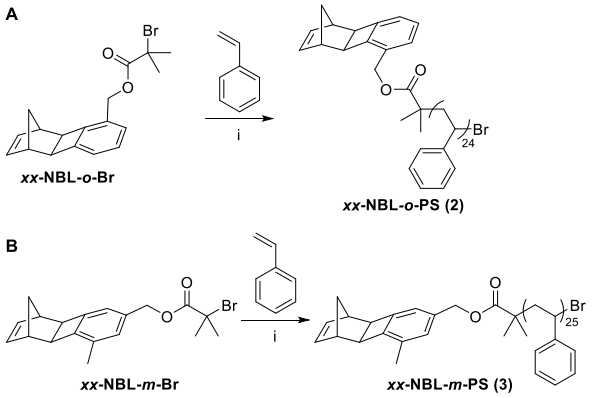

***xx*-NBL-*o*-PS (2)**: M_n = 2.9 kg/mol, $Đ$ = 1.04
***xx*-NBL-*m*-PS (3)**: M_n = 3.0 kg/mol, $Đ$ = 1.06

[a]Conditions: (i) Cu(I)Br, Cu(II)Br, PMDETA, 90 °C, 3 h.

With small-molecule monomer *xx*-NBL (**1**) and MMs *xx*-NBL-*o*-PS (**2**) and *xx*-NBL-*m*-PS (**3**) in hand, we studied the kinetics of ROMP for each in the synthesis of either linear or bottlebrush polymers. All polymerizations were initiated by G3 catalyst at rt and run open to air, at a monomer concentration of 20 mM in $CDCl_3$. Additionally, the catalyst to (macro)monomer ratio was controlled to target a DP of 100 for each polymerization. Aliquots were removed from all polymerizations at predetermined intervals and terminated with ethyl vinyl ether. For monomer *xx*-NBL (**1**), aliquots were then analyzed by ^{1}H NMR spectroscopy to measure monomer conversion by comparing the integration of the polymer backbone olefin protons to the monomer olefin protons (Figure S16). The final aliquot was also analyzed by SEC with differential refractive index (dRI) and multi-angle light scattering (MALS) detectors to determine M_n and $Đ$ values. For the two MMs, the solvent in each aliquot was evaporated quickly under a stream of air, and the residue was dissolved in tetrahydrofuran (THF) for SEC analysis. MM conversion was determined at each time point by comparing the areas under the MM and bottlebrush polymer peaks in the dRI traces (Figures S17–S18). Each polymerization was run at least three times, and the conversion data were then used to fit first-order kinetics plots for polymerization of monomer *xx*-NBL (**1**) and MMs *xx*-NBL-*o*-PS (**2**) and *xx*-NBL-*m*-PS (**3**) (Figure 1).

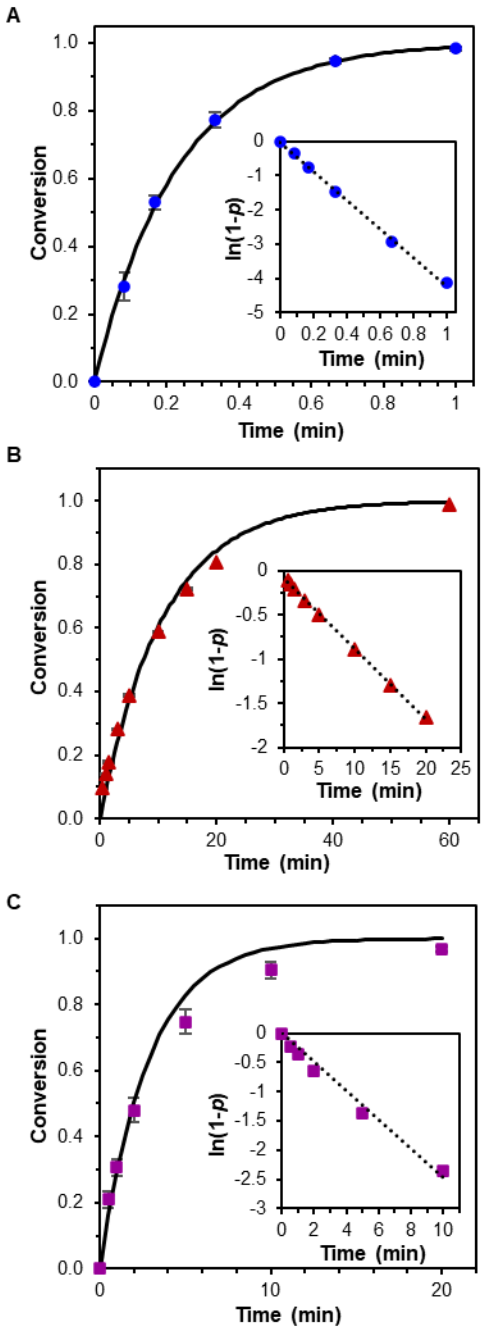

Figure 1. First-order ROMP kinetics analysis of (A) monomer *xx*-NBL (**1**), (B) MM *xx*-NBL-*o*-PS (**2**), and (C) MM *xx*-NBL-*m*-PS (**3**) in $CDCl_3$ at a [(macro)monomer]/[G3] ratio of 100:1 and [(macro)monomer] = 20 mM. Each experiment was run at least three times, and error bars show standard deviations. The solid line represents the fit to the averaged conversion data based on the equation $p = 1 - e^{(-k_{obs}t)}$ where p = fractional conversion.

All three (macro)monomers showed relatively good agreement between the conversion data and the first-order fits, although some deviation from the fit lines at high conversion was observed for the two MMs. We attribute this to an apparent influence of the degree of polymerization on k_p, where k_p decreases at high conversion due to the steric demands of the

growing bottlebrush macromolecule, a phenomenon we have observed previously.[49] Additionally, instead of reaching complete conversion, both MMs leveled off at 95% conversion based on SEC, even though ^{1}H NMR spectroscopy confirmed complete (>99%) consumption of the norbornene in all three cases. This phenomenon was previously observed in other norbornene MMs made by ATRP and is attributed to the presence of ~5% MM species that lack a norbornene end group.[58] Therefore, we adjusted the conversion data for MMs *xx*-NBL-*o*-PS (**2**) and *xx*-NBL-*m*-PS (**3**) to account for 5% MM species that lacked a norbornene (Figure 1B and 1C). Average $k_{p,obs}$ and propagation half-lives were calculated from the conversion versus time plots and are shown in Table 1.

Table 1. Summary of ROMP Kinetic Analysis of (Macro)Monomers

(Macro)monomer	$k_{p,obs}$[a] (min^{-1})	$t_{1/2}$ (min)	% conv[b]	Final $M_{n,expected}$[c] (kg/mol)	Final $M_{n,SEC}$[d] (kg/mol)	Final $Đ$[d]
xx-NBL (**1**)	4.4 ± 0.3	0.16 ± 0.01	>99	22	20	1.04
xx-NBL-*o*-PS (**2**)	0.094 ± 0.002	7.4 ± 0.2	95	276	244	1.06
xx-NBL-*m*-PS (**3**)	0.31 ± 0.04	2.3 ± 0.3	95	285	220	1.09

[a]Calculated from conversions measured by ^{1}H NMR spectroscopy (**1**) or SEC (**2**–**3**) on aliquots removed at specific time points during the polymerizations. A minimum of three polymerizations were run for each MM. [b]Measured on the final sample of the kinetics runs using ^{1}H NMR spectroscopy (**1**) by comparing the integrations of the polymer backbone olefin protons to the monomer olefin protons or using SEC (**2**–**3**) by comparing the areas of the bottlebrush polymer and MM peaks in the dRI trace (95% represents near-complete conversion for MMs **2**–**3** based on complete disappearance of the norbornene signal by ^{1}H NMR spectroscopy). [c]Determined using the equation $M_{n,expected} = M_{n,initial}$ * conv * $([MM]/[G3])_0$ where $M_{n,initial}$ is either the molecular weight of the monomer (**1**) or the $M_{n,SEC}$ measured for the MMs (**2**–**3**). [d]Measured on the final sample of the kinetics runs by SEC in THF at 30 °C with dRI and MALS detectors, using either the 100% mass recovery method to estimate d*n*/d*c* (**1**) or using the known d*n*/d*c* for PS of 0.185 mL/g (**2**–**3**).

All (macro)monomers reached near-complete conversion, and M_n values matched expected values while maintaining relatively low $Đ$ values for the final linear or bottlebrush polymer products. As expected, monomer *xx*-NBL (**1**) had a significantly higher $k_{p,obs}$ than both MMs; the $k_{p,obs}$ of monomer *xx*-NBL (**1**) was 14-fold higher than MM *xx*-NBL-*m*-PS (**3**) and almost 50-fold higher than MM *xx*-NBL-*o*-PS (**2**). This result is consistent with observations that k_p decreases with increasing side-chain molecular weight in MMs.[10, 59-60] Interestingly, the $k_{p,obs}$ values for the two MMs differed by a factor of 3.3, with MM *xx*-NBL-*m*-PS (**3**) polymerizing faster than MM *xx*-NBL-*o*-PS (**2**). This was surprising because the M_n values of the side-chains were the same and the anchor groups differed by only a methyl group aside from the regiochemistry on the arene ring.

The anchor group in these NBL compounds is quite rigid, preventing the mobility of the structural units close to the reactive norbornene olefin. We expected the rigidity of the anchor group to enhance k_p in ROMP compared with more common imide and ester-based anchor groups, because there would be less potential for steric interactions between the anchor group and the metal center. Additionally, we expected no chelation to the Ru center due to the lack of lone pairs in the (macro)monomers. These expectations were consistent for monomer *xx*-NBL (**1**) and MM *xx*-NBL-*m*-PS (**3**), which both exhibited high k_p values compared to other anchor groups.[48-49]

However, this expectation did not hold true for MM *xx*-NBL-*o*-PS (**2**), which exhibited an unexpectedly low k_p. Therefore, we surmised that the position of the PS side-chain on the arene ring was a pivotal factor influencing k_p in grafting-through ROMP of *xx*-NBL MMs.

Guironnet and coworkers found that the rate-determining step in ROMP is the formation of the metallacyclobutane ring.[47] In our previous work, we showed that the energy of the olefin-centered HOMO was a reasonable predictor of k_p because the rate-determining step employs the π electrons of the olefin substrate, corresponding to the HOMO, to form a bond with the catalyst.[46, 48-49] Therefore, we investigated the HOMO energies of the three *xx*-NBL (macro)monomers with electronic structure calculations. The HOMO energy for each (macro)monomer was calculated from optimized geometries using density functional theory (M06-2X method and def2-TZVP basis set).[61-62] For MMs *xx*-NBL-*o*-PS (**2**) and *xx*-NBL-*m*-PS (**3**), we used only one styrene unit to represent the entire PS side-chain. Our goal was to investigate the effects of the position of the side-chain on the HOMO, which should not be influenced by the side-chain beyond the first repeat unit. From these calculations, we found that monomer *xx*-NBL (**1**) had a HOMO energy of –174 kcal/mol and MMs *xx*-NBL-*o*-PS (**2**) and *xx*-NBL-*m*-PS (**3**) had HOMO energies of –178 and –177 kcal/mol, respectively. We then plotted these HOMO energies against the measured $k_{p,obs}$ values, including in the graphs several published norbornenes with various anchor groups, where HOMO energies were calculated using the same technique and $k_{p,obs}$ values were measured under identical conditions (Figure 2).

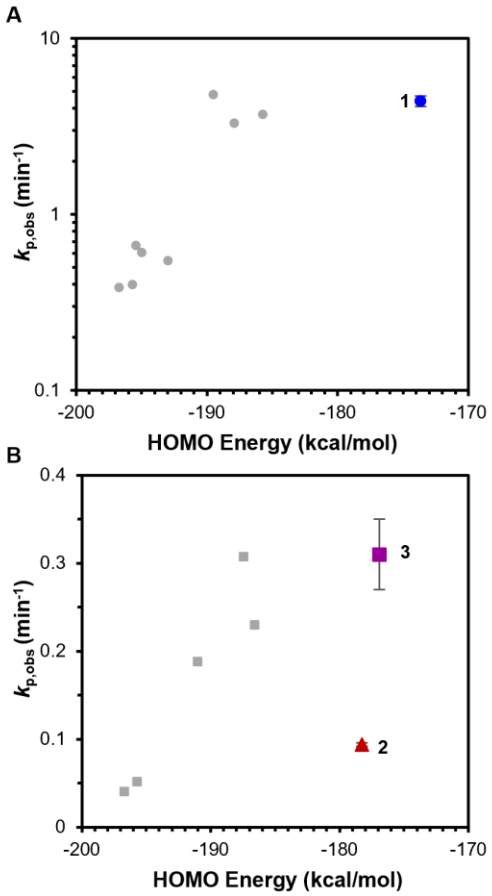

Figure 2. Measured $k_{p,obs}$ values versus HOMO energy for (A) monomer *xx*-NBL (**1**) (blue circle) compared to published small molecule *exo*-norbornene monomers with various anchor groups

(grey circles);[48] and (B) for MM *xx*-NBL-*o*-PS (**2**) (red triangle) and MM *xx*-NBL-*m*-PS (**3**) (purple square) compared to published MMs (grey squares).[49] Versions of these figures with structures for each of the grey points are shown in the Supporting Information (Figures S19–S20).

In our recently published work on the anchor group, monomers with higher HOMO energies had higher $k_{p,obs}$ values than monomers with lower HOMO energies.[48] Monomer *xx*-NBL (**1**) had a higher HOMO energy than the previously reported monomers by at least 10 kcal/mol but a $k_{p,obs}$ value similar to the fastest previously reported monomer. In other words, despite the much higher HOMO energy of monomer *xx*-NBL (**1**) compared to previously reported monomers, k_p did not increase, consistent with the plateau in k_p observed for monomers with HOMO energies greater than -190 kcal/mol in our previous study.[48] This plateau suggests that above a certain threshold, norbornene electronics no longer influences k_p, at least for small molecule monomers.

MMs *xx*-NBL-*o*-PS (**2**) and *xx*-NBL-*m*-PS (**3**) also had relatively high HOMO energies, –178 and –177 kcal/mol, respectively. When compared to MMs previously studied, MM *xx*-NBL-*m*-PS (**3**) had the highest HOMO energy and one of the highest $k_{p,obs}$ values, consistent with the positive correlation between HOMO energy and k_p. MM *xx*-NBL-*o*-PS (**2**) also had a higher HOMO energy than all previous MMs studied; however, the $k_{p,obs}$ of MM *xx*-NBL-*o*-PS (**2**) was unexpectedly low, aligning with MMs with low k_p anchor groups reported in the literature (i.e., *exo*-norbornene imide anchor groups).[49] This surprising discrepancy drew our attention to other potential factors affecting ROMP kinetics.

Our DFT calculations showed that the MM HOMO energies were 3–4 kcal/mol lower than that of monomer *xx*-NBL (1). This decrease in HOMO energy between the small molecule monomer and the MMs was surprising as previous studies showed very little difference, about 1 kcal/mol, in the HOMO energy when comparing monomer and MM structures containing the same anchor group. Thus, adding the polymer side-chain onto the *xx*-NBL anchor group changed the electronic structure of the MMs more so than other anchor groups previously studied. Additionally, the MM with the lowest $k_{p,obs}$, MM *xx*-NBL-*o*-PS (**2**), had the lowest HOMO energy, but it was only 1 kcal/mol lower than the HOMO energy for MM *xx*-NBL-*m*-PS (**3**). A difference of 1 kcal/mol in HOMO energy is likely within the error of the calculations and does not predict a large change in k_p between the two MMs, but we observed a 3.3-fold difference. This suggests that HOMO energy is not the only factor affecting the rate-determining step for MMs *xx*-NBL-*o*-PS (**2**) and *xx*-NBL-*m*-PS (**3**), further implying the importance of the position of the PS side-chain on the arene ring.

We hypothesized that the difference in propagation rates between MMs *xx*-NBL-*o*-PS (**2**) and *xx*-NBL-*m*-PS (**3**) might be explained by either i) an electronic difference between the two MMs, or ii) an effect of the orientation of the side-chains along the backbone. To test whether an electronic difference created the 3.3-fold difference in k_p values among the two MMs, we measured the rates of homopolymerization of the two ATRP initiators (compounds ***xx*-NBL-*o*-Br** and ***xx*-NBL-*m*-Br**, Figures S21–24). We anticipated that these α-bromoesters would have very similar electronic differences to the two MMs but without the complicating factor of the PS side-chains. The differences in the rates were negligible (Figure S25), indicating that electronic differences among the MMs do not explain the observed 3.3-fold difference in k_p values.

We then moved onto our second potential explanation for the observed k_p differences between the MMs, the orientation of the side-chains along the backbone. MMs experience steric effects during ROMP caused by the side-chains attached to the growing bottlebrush segment hindering unreacted MMs from approaching the Ru-center.[59] Therefore, changing the position of

the side-chains could lead to varying steric effects, resulting in the variable k_p values observed in MMs *xx*-NBL-*o*-PS (**2**) and *xx*-NBL-*m*-PS (**3**). Thus, we envisioned that the rate differences could be explained by examining the orientation of the side-chains relative to the reactive chain end.

An analysis of the propagating alkylidenes during ROMP of MM *xx*-NBL-*m*-PS (**3**) reveals that the number of bonds between the PS side-chain and the reactive chain end only changes by one for the two possible regioisomers (Scheme 4A). Therefore, during propagation, interactions between the PS side-chain and the Ru-center and ligands likely remain low regardless of which direction MM addition occurs. In contrast, the *ortho* position of the PS side-chain in MM *xx*-NBL-*o*-PS (**2**) makes the number of bonds between the reactive chain end and the side-chain lower than for MM *xx*-NBL-*m*-PS (**3**); when MM adds in one direction the side-chain is only 5 bonds away for the Ru-center (Scheme 4B). In this propagating alkylidene structure, the side-chain is more likely to sterically hinder the addition of new MM units, resulting in a lower k_p, than when the side-chain is oriented farther away from the Ru-center. Thus, during propagation the steric hindrance of MM addition for MM *xx*-NBL-*o*-PS (**2**) is likely higher than for MM *xx*-NBL-*m*-PS (**3**) because the *ortho* positioning causes the side-chains to be in closer proximity to the Ru-center and ligands than the *meta* positioning. Ultimately, this analysis suggests that the lower $k_{p,obs}$ found for MM *xx*-NBL-*o*-PS (**2**) compared to MM *xx*-NBL-*m*-PS (**3**) could be due to a greater steric effect for MM *xx*-NBL-*o*-PS (**2**), created by the *ortho* positioning of the side-chain, than that of MM *xx*-NBL-*m*-PS (**3**).

Scheme 4. Propagating alkylidene structures for MM *xx*-NBL-*m*-PS (**3**) (A) and MM *xx*-NBL-*o*-PS (**2**) (B).

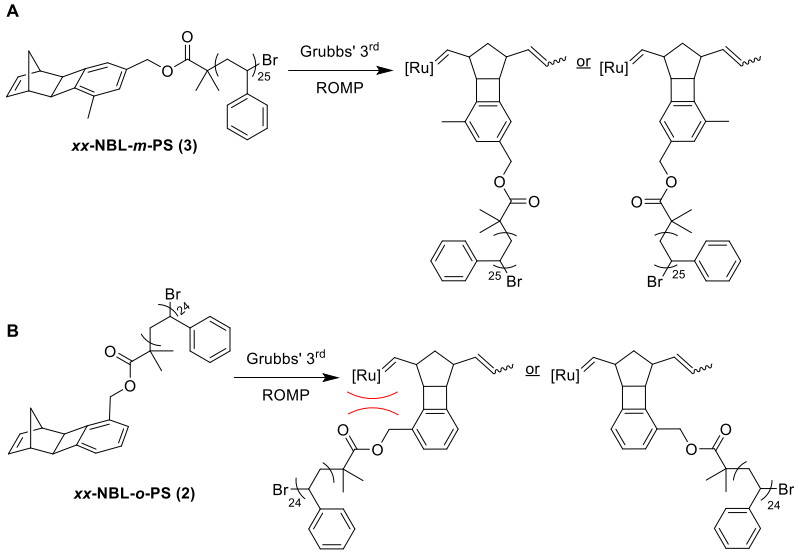

[a]The crowded environment near the Ru center in panel B (structure on left) suggests slow addition of the next MM *xx*-NBL-*o*-PS (**2**) unit.

To test this explanation for the observed rate differences, we copolymerized each MM with a small molecule diluent monomer to decrease the grafting density of the final bottlebrush polymer (Figure 3A). We predicted that spacing out the PS side-chains using a diluent monomer would lessen the steric interactions between the side-chains and the Ru-center for both MMs, resulting in nearly equal k_p values for the two MMs. We chose a diluent monomer, ***xx*-IM$_2$E'P**,[48] with a similar k_p to MM *xx*-NBL-*m*-PS (**3**) to avoid blocky compositions, with the expectation that the k_p of MM

xx-NBL-*o*-PS (**2**) would increase when polymerized with the diluent monomer compared to without the diluent monomer. We polymerized both MMs at rt and open to air, at a total norbornene concentration of 20 mM in $CDCl_3$. Again, the MM to catalyst ratio was set to 100, but 500 equiv of diluent monomer ***xx*-IM$_2$E'P** was included at the start of both polymerizations. Thus, the target grafting density was $z = 0.16$. Aliquots were removed from polymerizations at predetermined time intervals and terminated with ethyl vinyl ether before SEC analysis. MM conversion was determined at each time point by comparing the areas under the MM peak in the dRI traces normalized to an initial dRI trace before catalyst addition (Figures S26–S29). The conversion data were then used to fit first-order kinetics plots.

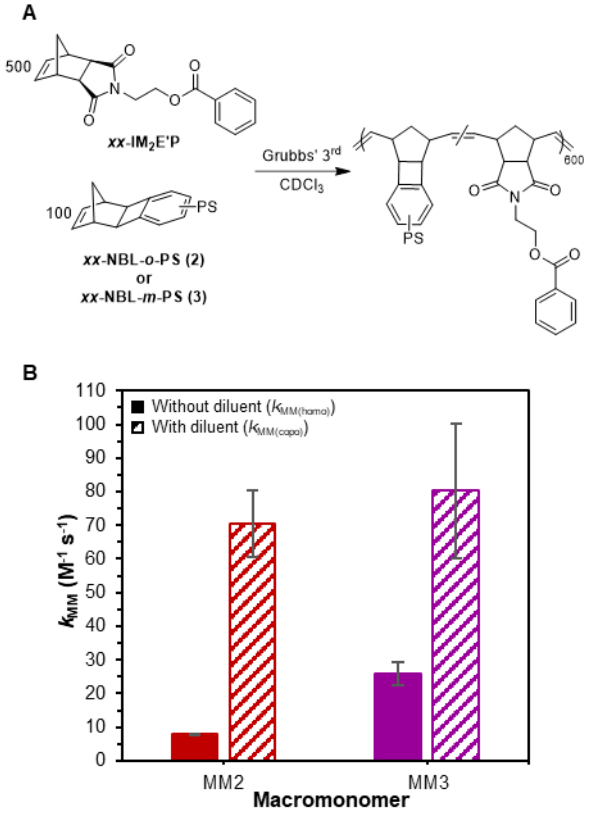

Figure 3. (A) Representative scheme for the copolymerization of either MM *xx*-NBL-*o*-PS (**2**) or *xx*-NBL-*m*-PS (**3**) with a diluent monomer, termed ***xx*-IM$_2$E'P**, to measure $k_{MM(copo)}$ values. Polymerizations were run at a total norbornene concentration of 20 mM in $CDCl_3$ under air at rt. (B) Measured propagation rate constant (k_{MM}) values for MMs *xx*-NBL-*o*-PS (**2**) and *xx*-NBL-*m*-PS (**3**) without diluent monomer, ($k_{MM(homo)}$, solid bars), and with diluent monomer ($k_{MM(copo)}$, patterned bars). Each experiment was repeated three times, and error bars show standard deviations.

Keeping the norbornene concentration at 20 mM, consistent with the homopolymerizations of the two MMs described above, resulted in a lower catalyst concentration than the homopolymerizations, but this was necessary to ensure proper stirring during ROMP. Therefore, we used second-order propagation rate constants (k_{MM}), which account for the difference in catalyst concentration, to compare the rate of MM addition during homopolymerization ($k_{MM(homo)}$) and copolymerization ($k_{MM(copo)}$). In comparing the k_{MM} values, we expected $k_{MM(copo)}$ to be higher

than $k_{MM(homo)}$ for both MMs due to the lower steric hinderance for each MM addition in the copolymerization studies.

The $k_{MM(homo)}$ of MM *xx*-NBL-*o*-PS (**2**) was 3.3-fold lower than that of MM *xx*-NBL-*m*-PS (**3**) under the same conditions, as discussed above. With the addition of diluent monomer, the $k_{MM(copo)}$ of both MMs *xx*-NBL-*o*-PS (**2**) and *xx*-NBL-*m*-PS (**3**) increased, consistent with our hypothesis that less side-chain interference would increase the rate of propagation when $z << 1$ (Figure 3B). As we hypothesized, the $k_{MM(copo)}$ values of the two MMs were nearly identical, varying by only 10% in these copolymerization studies, within the error of the measurement. In other words, MMs *xx*-NBL-*o*-PS (**2**) and *xx*-NBL-*m*-PS (**3**) polymerize at similar rates when $z <<1$, likely because the side-chain interactions during propagation are similar regardless of their positioning on the arene ring. Therefore, we conclude that $k_{MM(homo)}$ of MM *xx*-NBL-*o*-PS (**2**) is affected by the steric hinderance of the PS side-chains when $z = 1$, resulting in a lower $k_{MM(homo)}$ than MM *xx*-NBL-*m*-PS (**3**). These results support our hypothesis that the lower than expected k_p for MM 2, is due to the orientation of the PS side-chain during propagation.

Conclusions

In summary, we studied a new *exo*-norbornene anchor group termed *xx*-NBL in the form of a small molecule monomer and two PS MMs. The small molecule monomer structure had the highest HOMO energy and one of the highest k_p values compared to monomers previously reported. These findings support our previously stated hypothesis that higher norbornene HOMO energies increase k_p in ROMP of small molecule norbornene derivatives up to a certain level, above which the HOMO energy no longer affects the rate-determining step.[48] Interestingly, we observed a 3.3-fold difference in k_p between the two MMs due to the change in positioning of the polymer side-chain on the arene ring. We determined that the reactivity of these MM structures, predicted by HOMO energy, varied slightly due to the position of the side-chain, but not enough to explain the large difference in k_p. We hypothesized that the positioning of the PS side-chain changed the steric effects in ROMP such that side-chains closer to the reactive norbornene olefin (in the *ortho*-MM) hindered the addition of new MM units, slowing down polymerization compared to the *meta*-MM. When copolymerized with a diluent monomer, the rate of MM consumption only differed by 10% between the two MMs. We therefore conclude that copolymerization with a diluent monomer, resulting in $z << 1$, reduced the steric hinderance experienced by the *ortho*-MM, negating the rate differences observed between the two MMs in homopolymerization experiments. Ultimately, these *xx*-NBL (macro)monomers further broaden the scope of high k_p anchor group structures available for synthesizing complex polymer topologies such as bottlebrush polymers.

Acknowledgements

This work was supported by a joint grant between the National Science Foundation and the Binational Science Foundation (DMR-2104602) and by GlycoMIP, a National Science Foundation Materials Innovation Platform funded through Cooperative Agreement DMR-1933525. We thank Dr. Ryan Carrazzone and Ishani Sarkar for critically reading the manuscript. The authors acknowledge Advanced Research Computing at Virginia Tech for providing computational resources and technical support that have contributed to the results reported within this paper.

References

1. Blosch, S. E.; Scannelli, S. J.; Alaboalirat, M.; Matson, J. B., Complex Polymer Architectures Using Ring-Opening Metathesis Polymerization: Synthesis, Applications, and Practical Considerations. *Macromolecules* **2022**, *55*, 4200-4227.
2. Kim, K. H.; Nam, J.; Choi, J.; Seo, M.; Bang, J., From macromonomers to bottlebrush copolymers with sequence control: synthesis, properties, and applications. *Polym. Chem.* **2022**, *13*, 2224-2261.
3. Li, Z.; Tang, M.; Liang, S.; Zhang, M.; Biesold, G. M.; He, Y.; Hao, S.-M.; Choi, W.; Liu, Y.; Peng, J.; Lin, Z., Bottlebrush polymers: From controlled synthesis, self-assembly, properties to applications. *Prog. Polym. Sci.* **2021**, *116*, 101387.
4. Jha, S.; Dutta, S.; Bowden, N. B., Synthesis of Ultralarge Molecular Weight Bottlebrush Polymers Using Grubbs' Catalysts. *Macromolecules* **2004**, *37*, 4365-4374.
5. Sheiko, S. S.; Sumerlin, B. S.; Matyjaszewski, K., Cylindrical molecular brushes: Synthesis, characterization, and properties. *Prog. Polym. Sci.* **2008**, *33*, 759-785.
6. Verduzco, R.; Li, X.; Pesek, S. L.; Stein, G. E., Structure, function, self-assembly, and applications of bottlebrush copolymers. *Chem. Soc. Rev.* **2015**, *44*, 2405-2420.
7. Choi, T.-L.; Grubbs, R. H., Controlled Living Ring-Opening-Metathesis Polymerization by a Fast-Initiating Ruthenium Catalyst. *Angew. Chem* **2003**, *42*, 1743-1746.
8. Bielawski, C. W.; Grubbs, R. H., Living ring-opening metathesis polymerization. *Prog. Polym. Sci.* **2007**, *32*, 1-29.
9. Walsh, D. J.; Guironnet, D., Macromolecules with programmable shape, size, and chemistry. *Proc. Natl. Acad. Sci. U.S.A* **2019**, *116*, 1538-1542.
10. Ogbonna, N. D.; Dearman, M.; Cho, C.-T.; Bharti, B.; Peters, A. J.; Lawrence, J., Topologically Precise and Discrete Bottlebrush Polymers: Synthesis, Characterization, and Structure–Property Relationships. *JACS Au* **2022**, *2*, 898-905.
11. Nomura, K.; Schrock, R. R., Preparation of "Sugar-Coated" Homopolymers and Multiblock ROMP Copolymers. *Macromolecules* **1996**, *29*, 540-545.
12. Murphy, J. J.; Furusho, H.; Paton, R. M.; Nomura, K., Precise Synthesis of Poly(macromonomer)s Containing Sugars by Repetitive ROMP and Their Attachments to Poly(ethylene glycol): Synthesis, TEM Analysis and Their Properties as Amphiphilic Block Fragments. *Chemistry – A European Journal* **2007**, *13*, 8985-8997.
13. Kammeyer, J. K.; Blum, A. P.; Adamiak, L.; Hahn, M. E.; Gianneschi, N. C., Polymerization of protecting-group-free peptides via ROMP. *Polym. Chem.* **2013**, *4*, 3929-3933.
14. Sutthasupa, S.; Sanda, F.; Masuda, T., ROMP of Norbornene Monomers Carrying Nonprotected Amino Groups with Ruthenium Catalyst. *Macromolecules* **2009**, *42*, 1519-1525.
15. Xu, M.; Bullard, K. K.; Nicely, A. M.; Gutekunst, W. R., Resonance promoted ring-opening metathesis polymerization of twisted amides. *Chem. Sci.* **2019**, *10*, 9729-9734.
16. Medina, J. M.; Ko, J. H.; Maynard, H. D.; Garg, N. K., Expanding the ROMP Toolbox: Synthesis of Air-Stable Benzonorbornadiene Polymers by Aryne Chemistry. *Macromolecules* **2017**, *50*, 580-586.

17. Hancock, S. N.; Yuntawattana, N.; Valdez, S. M.; Michaudel, Q., Expedient synthesis and ring-opening metathesis polymerization of pyridinonorbornenes. *Polym. Chem.* **2022**, *13*, 5530-5535.
18. Nguyen, H. V. T.; Gallagher, N. M.; Vohidov, F.; Jiang, Y.; Kawamoto, K.; Zhang, H.; Park, J. V.; Huang, Z.; Ottaviani, M. F.; Rajca, A.; Johnson, J. A., Scalable Synthesis of Multivalent Macromonomers for ROMP. *ACS Macro Lett.* **2018**, *7*, 472-476.
19. Dutertre, F.; Bang, K.-T.; Vereroudakis, E.; Loppinet, B.; Yang, S.; Kang, S.-Y.; Fytas, G.; Choi, T.-L., Conformation of Tunable Nanocylinders: Up to Sixth-Generation Dendronized Polymers via Graft-Through Approach by ROMP. *Macromolecules* **2019**, *52*, 3342-3350.
20. Fu, L.; Sui, X.; Crolais, A. E.; Gutekunst, W. R., Modular Approach to Degradable Acetal Polymers Using Cascade Enyne Metathesis Polymerization. *Angew. Chem* **2019**, *58*, 15726-15730.
21. Mandal, A.; Mandal, I.; Kilbinger, A. F. M., Catalytic Syntheses of Degradable Polymers via Ring-Opening Metathesis Copolymerization Using Vinyl Ethers as Chain Transfer Agents. *Macromolecules* **2022**, *55*, 7827-7833.
22. Boadi, F. O.; Zhang, J.; Yu, X.; Bhatia, S. R.; Sampson, N. S., Alternating Ring-Opening Metathesis Polymerization Provides Easy Access to Functional and Fully Degradable Polymers. *Macromolecules* **2020**, *53*, 5857-5868.
23. Chae, C.-G.; Yu, Y.-G.; Seo, H.-B.; Kim, M.-J.; Kishore, M. Y. L. N.; Lee, J.-S., Molecular and kinetic design for the expanded control of molecular weights in the ring-opening metathesis polymerization of norbornene-substituted polyhedral oligomeric silsesquioxanes. *Polym. Chem.* **2018**, *9*, 5179-5189.
24. Yu, H.; Lin, S.; Sun, D.; Pan, Q., Synthesis of norbornene derivatives and their polymers via ROMP of norbornene derivatives. *High Performance Polymers* **2020**, *32*, 729-737.
25. Wolf, W. J.; Lin, T.-P.; Grubbs, R. H., Examining the Effects of Monomer and Catalyst Structure on the Mechanism of Ruthenium-Catalyzed Ring-Opening Metathesis Polymerization. *J. Am. Chem. Soc.* **2019**, *141*, 17796-17808.
26. Lu, P.; Kensy, V. K.; Tritt, R. L.; Seidenkranz, D. T.; Boydston, A. J., Metal-Free Ring-Opening Metathesis Polymerization: From Concept to Creation. *Acc. Chem. Res.* **2020**, *53*, 2325-2335.
27. Archer, W. R.; Dinges, G. E.; MacNicol, P. L.; Schulz, M. D., Synthesis of bottlebrush polymers based on poly(N-sulfonyl aziridine) macromonomers. *Polym. Chem.* **2022**, *13*, 6134-6139.
28. Xiao, L.; Qu, L.; Zhu, W.; Wu, Y.; Liu, Z.; Zhang, K., Donut-Shaped Nanoparticles Templated by Cyclic Bottlebrush Polymers. *Macromolecules* **2017**, *50*, 6762-6770.
29. Müllner, M.; Lunkenbein, T.; Schieder, M.; Gröschel, A. H.; Miyajima, N.; Förtsch, M.; Breu, J.; Caruso, F.; Müller, A. H. E., Template-Directed Mild Synthesis of Anatase Hybrid Nanotubes within Cylindrical Core–Shell–Corona Polymer Brushes. *Macromolecules* **2012**, *45*, 6981-6988.
30. Aviv, Y.; Altay, E.; Fink, L.; Raviv, U.; Rzayev, J.; Shenhar, R., Quasi-Two-Dimensional Assembly of Bottlebrush Block Copolymers with Nanoparticles in Ultrathin Films: Combined Effect of Graft Asymmetry and Nanoparticle Size. *Macromolecules* **2019**, *52*, 196-207.
31. Miyake, G. M.; Weitekamp, R. A.; Piunova, V. A.; Grubbs, R. H., Synthesis of Isocyanate-Based Brush Block Copolymers and Their Rapid Self-Assembly to Infrared-Reflecting Photonic Crystals. *J. Am. Chem. Soc.* **2012**, *134*, 14249-14254.

32. Macfarlane, R. J.; Kim, B.; Lee, B.; Weitekamp, R. A.; Bates, C. M.; Lee, S. F.; Chang, A. B.; Delaney, K. T.; Fredrickson, G. H.; Atwater, H. A.; Grubbs, R. H., Improving Brush Polymer Infrared One-Dimensional Photonic Crystals via Linear Polymer Additives. *J. Am. Chem. Soc.* **2014**, *136*, 17374-17377.
33. Boyle, B. M.; French, T. A.; Pearson, R. M.; McCarthy, B. G.; Miyake, G. M., Structural Color for Additive Manufacturing: 3D-Printed Photonic Crystals from Block Copolymers. *ACS Nano* **2017**, *11*, 3052-3058.
34. Thompson, K. A.; Mayder, D. M.; Tonge, C. M.; Sauvé, E. R.; Lefeaux, H. R.; Hudson, Z. M., A grafting-from strategy for the synthesis of bottlebrush nanofibers from organic semiconductors. *Can. J. Chem.* **2023**, *101*, 118-125.
35. Yin, X.; Qiao, Y.; Gadinski, M. R.; Wang, Q.; Tang, C., Flexible thiophene polymers: a concerted macromolecular architecture for dielectrics. *Polym. Chem.* **2016**, *7*, 2929-2933.
36. Tonge, C. M.; Sauvé, E. R.; Cheng, S.; Howard, T. A.; Hudson, Z. M., Multiblock Bottlebrush Nanofibers from Organic Electronic Materials. *J. Am. Chem. Soc.* **2018**, *140*, 11599-11603.
37. Self, J. L.; Sample, C. S.; Levi, A. E.; Li, K.; Xie, R.; de Alaniz, J. R.; Bates, C. M., Dynamic Bottlebrush Polymer Networks: Self-Healing in Super-Soft Materials. *J. Am. Chem. Soc.* **2020**, *142*, 7567-7573.
38. Arrington, K. J.; Radzinski, S. C.; Drummey, K. J.; Long, T. E.; Matson, J. B., Reversibly Cross-linkable Bottlebrush Polymers as Pressure-Sensitive Adhesives. *ACS Appl. Mater. Interfaces* **2018**, *10*, 26662-26668.
39. Fournier, L.; Rivera Mirabal, D. M.; Hillmyer, M. A., Toward Sustainable Elastomers from the Grafting-Through Polymerization of Lactone-Containing Polyester Macromonomers. *Macromolecules* **2022**, *55*, 1003-1014.
40. Lienkamp, K.; Madkour, A. E.; Musante, A.; Nelson, C. F.; Nüsslein, K.; Tew, G. N., Antimicrobial Polymers Prepared by ROMP with Unprecedented Selectivity: A Molecular Construction Kit Approach. *J. Am. Chem. Soc.* **2008**, *130*, 9836-9843.
41. Zhao, P.; Liu, L.; Feng, X.; Wang, C.; Shuai, X.; Chen, Y., Molecular Nanoworm with PCL Core and PEO Shell as a Non-spherical Carrier for Drug Delivery. *Macromol. Rapid Commun.* **2012**, *33*, 1351-1355.
42. Miki, K.; Kimura, A.; Oride, K.; Kuramochi, Y.; Matsuoka, H.; Harada, H.; Hiraoka, M.; Ohe, K., High-Contrast Fluorescence Imaging of Tumors In Vivo Using Nanoparticles of Amphiphilic Brush-Like Copolymers Produced by ROMP. *Angew. Chem* **2011**, *50*, 6567-6570.
43. Vohidov, F.; Milling, L. E.; Chen, Q.; Zhang, W.; Bhagchandani, S.; Nguyen, Hung V. T.; Irvine, D. J.; Johnson, J. A., ABC triblock bottlebrush copolymer-based injectable hydrogels: design, synthesis, and application to expanding the therapeutic index of cancer immunochemotherapy. *Chem. Sci.* **2020**, *11*, 5974-5986.
44. Detappe, A.; Nguyen, H. V. T.; Jiang, Y.; Agius, M. P.; Wang, W.; Mathieu, C.; Su, N. K.; Kristufek, S. L.; Lundberg, D. J.; Bhagchandani, S.; Ghobrial, I. M.; Ghoroghchian, P. P.; Johnson, J. A., Molecular bottlebrush prodrugs as mono- and triplex combination therapies for multiple myeloma. *Nature Nanotechnology* **2023**, *18*, 184-192.
45. Slugovc, C.; Demel, S.; Riegler, S.; Hobisch, J.; Stelzer, F., The Resting State Makes the Difference: The Influence of the Anchor Group in the ROMP of Norbornene Derivatives. *Macromol. Rapid Commun.* **2004**, *25*, 475-480.

46. Radzinski, S. C.; Foster, J. C.; Chapleski, R. C.; Troya, D.; Matson, J. B., Bottlebrush Polymer Synthesis by Ring-Opening Metathesis Polymerization: The Significance of the Anchor Group. *J. Am. Chem. Soc.* **2016**, *138*, 6998-7004.
47. Hyatt, M. G.; Walsh, D. J.; Lord, R. L.; Andino Martinez, J. G.; Guironnet, D., Mechanistic and Kinetic Studies of the Ring Opening Metathesis Polymerization of Norbornenyl Monomers by a Grubbs Third Generation Catalyst. *J. Am. Chem. Soc.* **2019**, *141*, 17918-17925.
48. Scannelli, S. J.; Paripati, A.; Weaver, J. R.; Vu, C.; Alaboalirat, M.; Troya, D.; Matson, J. B., Influence of the Norbornene Anchor Group in Ru-Mediated Ring-Opening Metathesis Polymerization: Synthesis of Linear Polymers. *Macromolecules* **2023**, *56*, 3848-3856.
49. Scannelli, S. J.; Alaboalirat, M.; Troya, D.; Matson, J. B., Influence of the Norbornene Anchor Group in Ru-Mediated Ring-Opening Metathesis Polymerization: Synthesis of Bottlebrush Polymers. *Macromolecules* **2023**, *56*, 3838-3847.
50. Liu, S.; Jin, Z.; Teo, Y. C.; Xia, Y., Efficient Synthesis of Rigid Ladder Polymers via Palladium Catalyzed Annulation. *J. Am. Chem. Soc.* **2014**, *136*, 17434-17437.
51. Jin, Z.; Teo, Y. C.; Zulaybar, N. G.; Smith, M. D.; Xia, Y., Streamlined Synthesis of Polycyclic Conjugated Hydrocarbons Containing Cyclobutadienoids via C–H Activated Annulation and Aromatization. *J. Am. Chem. Soc.* **2017**, *139*, 1806-1809.
52. Lai, H. W. H.; Teo, Y. C.; Xia, Y., Functionalized Rigid Ladder Polymers from Catalytic Arene-Norbornene Annulation Polymerization. *ACS Macro Lett.* **2017**, *6*, 1357-1361.
53. Lai, H. W. H.; Liu, S.; Xia, Y., Norbornyl benzocyclobutene ladder polymers: Conformation and microporosity. *J. Polym. Sci., Part A: Polym. Chem.* **2017**, *55*, 3075-3081.
54. Rule, J. D.; Moore, J. S., ROMP Reactivity of endo- and exo-Dicyclopentadiene. *Macromolecules* **2002**, *35*, 7878-7882.
55. Ivin, K. J.; Mol, J. C., 11 - Ring-Opening Metathesis Polymerization: General Aspects. In *Olefin Metathesis and Metathesis Polymerization (Second Edition)*, Ivin, K. J.; Mol, J. C., Eds. Academic Press: London, 1997; pp 224-259.
56. Alaboalirat, M.; Vu, C.; Matson, J. B., Radical–radical coupling effects in the direct-growth grafting-through synthesis of bottlebrush polymers using RAFT and ROMP. *Polym. Chem.* **2022**, *13*, 5841-5851.
57. Naguib, M.; Nixon, K. L.; Keddie, D. J., Effect of radical copolymerization of the (oxa)norbornene end-group of RAFT-prepared macromonomers on bottlebrush copolymer synthesis via ROMP. *Polym. Chem.* **2022**, *13*, 1401-1410.
58. Blosch, S. E.; Alaboalirat, M.; Eades, C. B.; Scannelli, S. J.; Matson, J. B., Solvent Effects in Grafting-through Ring-Opening Metathesis Polymerization. *Macromolecules* **2022**, *55*, 3522-3532.
59. Ren, N.; Yu, C.; Zhu, X., Topological Effect on Macromonomer Polymerization. *Macromolecules* **2021**, *54*, 6101-6108.
60. Zografos, A.; Lynd, N. A.; Bates, F. S.; Hillmyer, M. A., Impact of Macromonomer Molar Mass and Feed Composition on Branch Distributions in Model Graft Copolymerizations. *ACS Macro Lett.* **2021**, *10*, 1622-1628.
61. Zhao, Y.; Truhlar, D. G., The M06 suite of density functionals for main group thermochemistry, thermochemical kinetics, noncovalent interactions, excited states, and transition elements: two new functionals and systematic testing of four M06-class functionals and 12 other functionals. *Theor. Chem. Acc,* **2008**, *120*, 215-241.

62. Weigend, F.; Ahlrichs, R., Balanced basis sets of split valence, triple zeta valence and quadruple zeta valence quality for H to Rn: Design and assessment of accuracy. *Phys. Chem. Chem. Phys.* **2005**, *7*, 3297-3305.